Eur. Phys. J. D **22**, 311–317 (2003)
DOI: 10.1140/epjd/e2002-00228-6

THE EUROPEAN PHYSICAL JOURNAL D

Pump-probe spectroscopy of atoms cooled in a 3D lin⊥lin optical lattice

F.-R. Carminati, M. Schiavoni, Y. Todorov, F. Renzoni[a], and G. Grynberg

Laboratoire Kastler Brossel, Département de Physique de l'École Normale Supérieure, 24 rue Lhomond, 75231 Paris Cedex 05, France

Received 8 April 2002 / Received in final form 9 September 2002
Published online 12 November 2002 –

Abstract. We describe the pump-probe spectroscopy of atoms cooled in a 3D lin⊥lin optical lattice. Our pump-probe configuration consists of two laser fields detuned with respect to the lattice fields. This scheme allows to clearly identify in the probe transmission spectrum the Brillouin and Raman resonances, by studying their positions as functions of the angle between the pump and probe beams. We describe these resonances in detail, and compare the experimental results to the theoretical predictions. Our conclusions are supported by transport-spectroscopy measurements, which allow to distinguish between contributions to the light scattering from propagating and non-propagating atoms.

PACS. 05.45.-a Nonlinear dynamics and nonlinear dynamical systems – 42.65.Es Stimulated Brillouin and Rayleigh scattering – 32.80.Pj Optical cooling of atoms; trapping

1 Introduction

Stimulated light scattering is a powerful technique to investigate the properties of a medium, as well for solids and samples in the vapour phase. It allows not only to determine the dynamical modes of the sample, but also to study the relaxation processes towards equilibrium. In the last decade the methods of stimulated light scattering have found wide application in the domain of cold atoms [1–10]. For example the oscillation frequencies of atoms bound by an external optical potential can be precisely determined by measuring the position of Raman lines in the nonlinear optical response of the atomic sample [1]. And if the atoms are instead free, stimulated light scattering between different motional states allows to determine their velocity distribution [5–9]. In this work we present a detailed investigation of the nonlinear optical response of atoms cooled in an optical lattice [11]. At variance with previous investigations [1,4], in which the light scattering was established between a probe beam and the lattice beams, in our scheme the photons are scattered between a probe and an additional pump beam. As it will be shown, this results in a complete freedom in the choice of the mode of the material medium to be excited, and allows the experimental verification of properties of optical lattices so far assumed but not demonstrated. In particular we will show that the considered pump-probe configuration allows to clearly identify in the probe transmission spectrum the Brillouin and Raman resonances, by studying their positions as functions of the angle between the pump and probe beams. This study also offers a striking evidence of the completely different nature of these resonances. Our conclusions are supported by transport-spectroscopy measurements: the velocity of the center of mass of the atomic cloud is monitored as a function of the detuning between pump and probe. This offers an alternative way to distinguish between contributions to the light scattering from propagating and non-propagating atoms.

The results presented in this work are obtained for a dissipative optical lattice. However, we note that, as the pump and probe fields can be arbitrarily detuned from atomic resonance, the described methods of pump-probe spectroscopy can be applied also to far-off-resonance non-dissipative optical lattices which are currently investigated by many groups in connection with Bose-Einstein condensation experiments [12].

This work is organized as follows. In Section 2 we describe the experimental set-up. In Section 3 we analyze the pump-probe configuration with parallel polarizations of the beams. In the configuration of Section 4, the polarizations of the pump and probe beams are instead orthogonal. In each of Sections 3 and 4 the Rayleigh, Raman and Brillouin (when presents) resonances are examined separately. With respect to the scheme with only one additional probe beam, the pump-probe configuration examined here offers significative advantages for the study of the Raman and Brillouin resonances, but not for the Rayleigh lines. Therefore the discussion of these latter will be kept to a minimum. The conclusions of our work are contained in Section 5.

[a] e-mail: Ferruccio.Renzoni@lkb.ens.fr

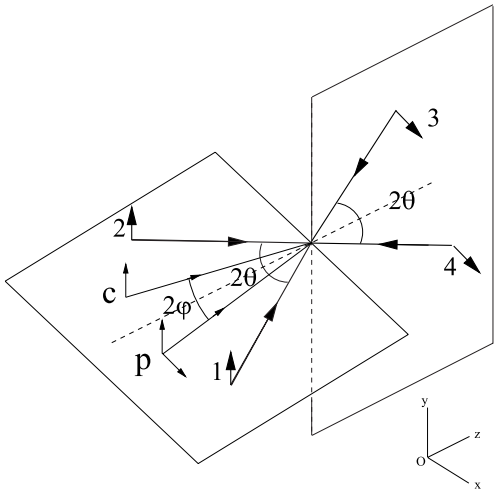

Fig. 1. Laser fields configuration for the 3D lin⊥lin optical lattice. The beams 1–4 generate the static 3D periodic potential. For the measurement presented in this work, the angles between the lattice beams are kept fixed at $\theta = 30^\circ$. Two additional laser beams (c and p), are introduced for the pump-probe spectroscopy. The pump beam (c) is linearly polarized along the y-axis. For the probe beam (p), both configurations with polarization along the y-axis and in the xOz-plane have been considered in the experiment.

2 Experimental set-up

In our experiment ^{85}Rb atoms are cooled and trapped in a 3D lin⊥lin optical lattice. The procedure to load the atoms in the optical lattice is the standard one used in previous experiments [7]. The rubidium atoms are first cooled and trapped in a magneto-optical trap (MOT). Then the MOT magnetic field and laser beams are turned off and the lattice beams are turned on.

The three-dimensional periodic structure is generated by the interference of four linearly polarized laser beams, arranged in the 3D lin⊥lin configuration [11] (Fig. 1): two y-polarized beams propagate in the xOz-plane with a relative angle 2θ, while two x-polarized beams propagate in the yOz-plane and form also an angle 2θ. This arrangement results in a periodic modulation of the light polarization and light intensity, which produces a periodic modulation of the different atomic ground-state sublevels (optical potentials). The optical potential has minima located on a orthorhombic lattice and associated with pure circular (alternatively σ^+ and σ^-) polarization. The lattice constants, *i.e.* the distance (along a major axis) between two sites of equal circular polarization are $\lambda_{x,y} = \lambda/\sin\theta$ and $\lambda_z = \lambda/(2\cos\theta)$, with λ the laser field wavelength. The optical pumping between the different atomic ground states combined with the spatial modulation of the light shifts leads then to the cooling of atoms [13] and to their localization [14] at the minima of the optical potential, thus producing a periodic array of atoms.

After 10 ms of thermalization of the atoms in the optical lattice, two additional linearly-polarized laser fields are introduced for the pump-probe spectroscopy. The strong pump (or coupling) beam is kept at a given frequency, while the frequency of the weak probe beam is scanned around the pump frequency. The relative detuning between pump and probe is indicated by δ_{pc}:

$$\delta_{pc} = \omega_p - \omega_c, \tag{1}$$

and analogously for the $\mathbf{k}$-vectors difference $\Delta\mathbf{k}_{pc}$:

$$\Delta\mathbf{k}_{pc} = \mathbf{k}_p - \mathbf{k}_c. \tag{2}$$

The pump and probe beams are detuned with respect to the lattice beams, so that there is no atomic observable which can be excited at the beat frequency. Furthermore as the pump and probe fields are derived from a laser different from the one producing the lattice beams, the effect of the unwanted beat is significantly reduced.

3 Configuration with y-polarized pump and probe

We consider first a configuration with the pump and the probe beams linearly polarized along the y-axis, *i.e.* with polarizations parallel to those of the copropagating lattice beams. They propagate in the xOz-plane and they are symmetrically displaced with respect to the z-axis. The angle between the two beams is denoted by 2φ (Fig. 1). As it will be shown rigorously in the following, this configuration corresponds to excitations in the x-direction.

We measured the probe transmission as a function of the detuning δ_{pc} for different angles between the pump and the probe beams, with results as the ones shown in Figure 2. The probe transmission spectrum shows up to five resonances. The position of these resonances, as well their number, depends on the angle between the pump and the probe beams. A resonance centered at zero detuning is present in all the spectra. At small angle φ two lateral resonances of opposite sign are also present. The position of these resonances, marked with arrows in Figure 2, is found to be an increasing function of the angle φ. At larger values of φ, two additional lateral resonances appear, their position (dotted lines in Fig. 2) being independent of the angle φ.

We have also made transport-spectroscopy measurements, by taking images of the atomic cloud at different time instants. For these measurements we increased the power of the probe field so to have about the same intensity in the pump and probe beams. From the images, we derived the velocity of the center-of-mass of the atomic cloud as a function of δ_{pc}. As shown in Figure 3, two resonances of opposite sign and symmetrically displaced with respect to $\delta_{pc} = 0$ are present in the spectrum for the x-component of the center-of-mass velocity. The measurements show that the position of these resonances depends clearly on the angle φ between pump and probe. By contrast, we found that the z-component (not shown in the figure) of the center-of-mass velocity does not show any resonant behaviour with δ_{pc}. We analyze all these resonances in detail in the following.

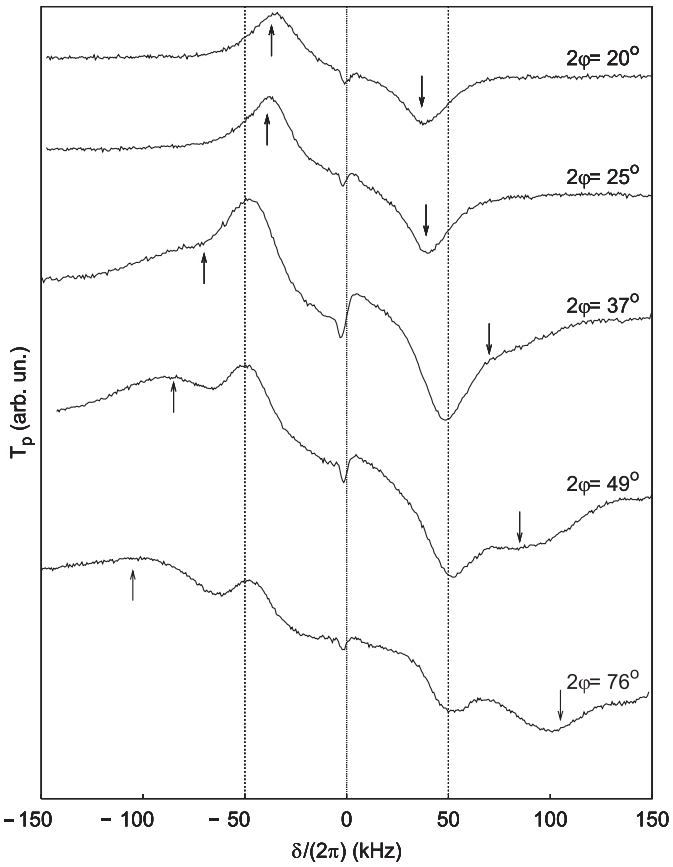

Fig. 2. Transmission of the probe beam as a function of the detuning between pump and probe fields, for different values of the angle 2φ between pump and probe beams. The lattice detuning is $\Delta = -50$ MHz, the intensity per lattice beam $I_L = 5$ mW/cm^2. The intensity of the pump and probe beams are: $I_c \simeq 0.5$ mW/cm^2, $I_p \simeq 0.1$ mW/cm^2.

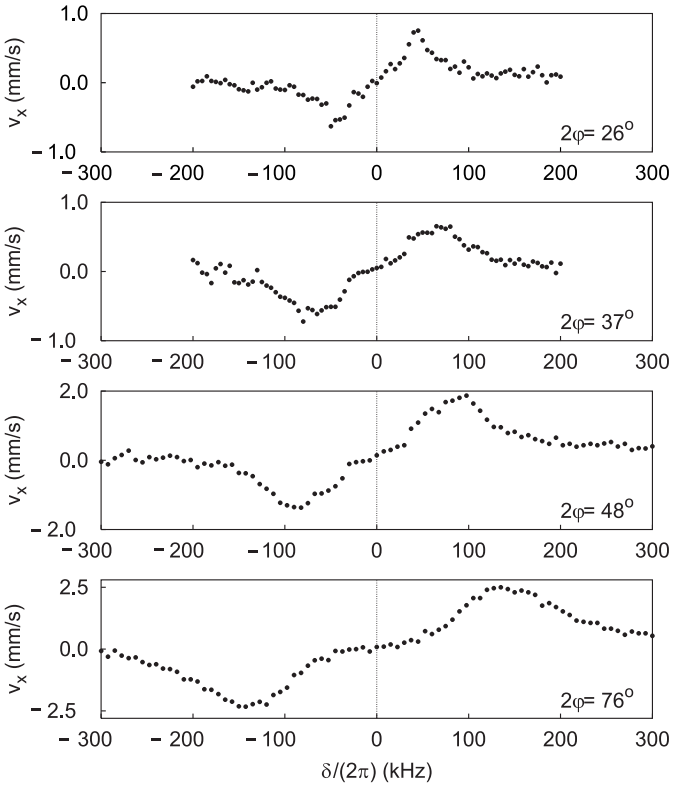

Fig. 3. Center-of-mass velocity in the x-direction as a function of the detuning between pump and probe fields, for different values of the angle 2φ between pump and probe beams. The lattice detuning is $\Delta = -50$ MHz, the intensity per lattice beam $I_L = 5$ mW/cm^2.

3.1 Rayleigh resonances

The resonance at the center of the spectrum corresponds to stimulated Rayleigh scattering. These resonances originate from the diffraction of the pump on the phase-shifted modulation of an observable of the atomic medium [15]. Indeed the interference between pump and probe fields results in a pattern moving at a phase velocity

$$v_\phi = \frac{\delta_{pc}}{|\Delta \mathbf{k}_{pc}|} = \frac{\delta_{pc}}{2k \sin \varphi} \tag{3}$$

($|\mathbf{k}_c| \simeq |\mathbf{k}_p| \equiv k$). This interference pattern creates a modulation of one (or more) atomic observable moving at the same velocity v_ϕ but phase-shifted with respect to the light interference pattern. This phase shift originates from the finite response time of the material medium. As the light interference pattern and the material grating are phase shifted, the pump wave can be diffracted on the grating in the direction of the probe thus modifying the probe transmission.

In the present configuration with parallel polarizations of the pump and probe beams, it is the light intensity which is periodically modulated. Previous work (see [11] and references therein) identified in the atomic density the material observable which, excited *via* the dipole force, is responsible for the Rayleigh line.

Rayleigh resonances are usually known to be dispersive-like [15]. However in the present case of Rayleigh resonances in optical lattices, the radiation pressure results in a Lorentzian contribution. This has been studied in detail in reference [16], and it will not be repeated here.

3.2 Raman resonances

The lateral resonances at $\delta_{pc} \simeq \pm 2\pi \times 50$ kHz correspond to Raman transitions between different vibrational levels of the same potential well (Fig. 4). The sign of these resonances is easily understood by taking into account the equilibrium population distribution produced by the cooling process [14]. As the ground vibrational level is more populated than the first excited one, in the Raman process between these two states it will be the field with lower energy to be amplified. To negative detunings $\delta_{pc} < 0$ corresponds then probe gain, and to $\delta_{pc} > 0$ probe attenuation.

To determine which transition is excited for a given pump-probe configuration, *i.e.* for a given difference $\Delta \mathbf{k}_{pc}$

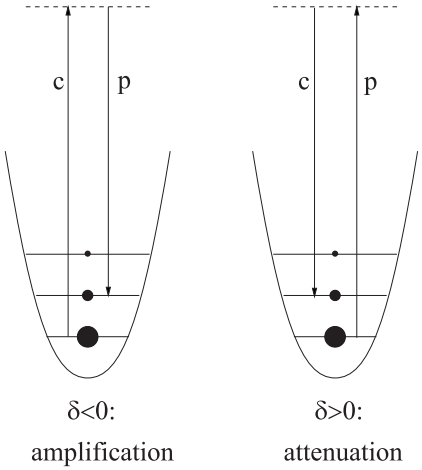

Fig. 4. Raman transitions between different vibrational levels of the same potential well. The solid circles indicate the population distribution in the different levels.

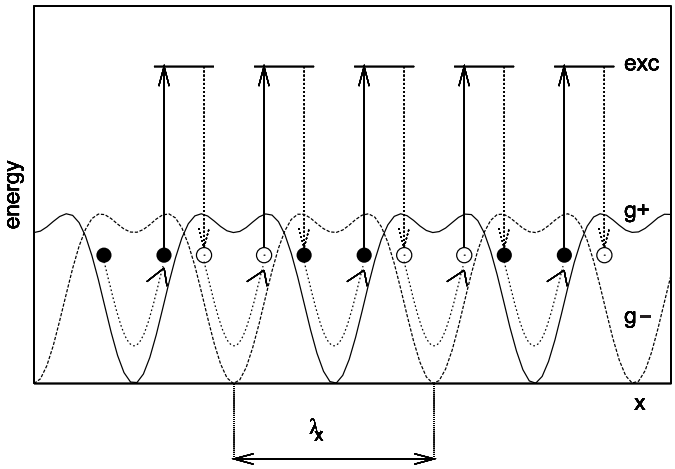

Fig. 5. Atomic trajectory corresponding to a Brillouin mode in the x-direction. The shown potential curves (g_+ and g_-) are the section along $y = z = 0$ of the optical potential for a $J_g = 1/2 \rightarrow J_e = 3/2$ atomic transition and a 3D lin⊥lin beam configuration.

between the pump and the probe wavevectors, we should calculate the matrix elements of the Raman operator $I = (\mathbf{d} \cdot \mathbf{E}_c^\dagger)(\mathbf{d} \cdot \mathbf{E}_p)$ between different vibrational states. Here $\mathbf{d}$ is the atomic dipole operator, and $\mathbf{E}_\alpha$ ($\alpha = c, p$) the electric field operators.

As we are considering atomic states well localized near the bottom of a potential well, we can describe the optical potential as a 3D harmonic oscillator and label the vibrational states accordingly: $|\{n\}\rangle = |\{n_x, n_y, n_z\}\rangle$. The internal ground and excited atomic states will be labeled as $|J_g, m_g\rangle$ and $|J_e, m_e\rangle$, for a quantization axis in the z-direction. The Raman process induces transitions between ground states with the same quantum number m_g. The basic step in the calculation of the matrix element $I_{nn'}$ of the Raman operator is the expansion of the pump and probe electric fields near the bottom of the potential well (say $\mathbf{r} = \mathbf{0}$)

$$\exp\{\mathrm{i}(\mathbf{k}_p - \mathbf{k}_c) \cdot \mathbf{r}\} \simeq 1 + \mathrm{i}\Delta\mathbf{k}_{pc} \cdot \mathbf{r}. \tag{4}$$

After elementary calculations we obtain for $n \neq n'$

$$I_{nn'} \simeq \frac{\mathrm{i}(c_- + c_+)\mathcal{D}^2 \mathcal{E}_c^{o*} \mathcal{E}_p^o}{2(2J_e + 1)} \langle\{n'\}|\mathbf{r}|\{n\}\rangle \cdot \Delta\mathbf{k}_{pc}. \tag{5}$$

Here $c_\pm = \langle J_e, m_g \pm 1 | J_g, 1; m_g, \pm 1\rangle^2$, $\mathcal{D}$ is the reduced matrix element of the dipole operator, and $\mathcal{E}_c^o$, $\mathcal{E}_p^o$ are the amplitudes of the pump and probe beams.

Equation (5) shows that the coupling is of the form $\Delta\mathbf{k}_{pc} \cdot \mathbf{r}$. This means that for a pump-probe configuration leading to a $\Delta\mathbf{k}_{pc}$ in the x-direction, as in our case, only Ω_x-resonances ($\Delta n_x = \pm 1$, $\Delta n_{y,z} = 0$) will be excited, and analogously for the other possible orientation of $\Delta\mathbf{k}_{pc}$. It is then clear that an appropriate choice of $\Delta\mathbf{k}_{pc}$, *i.e.* of the displacement of the pump and probe fields, allows the excitation of the Raman resonance in any desired direction. Furthermore the proportionality of the matrix element of the Raman operator to $\Delta\mathbf{k}_{pc}$ implies that the transition rate is proportional to $\sin^2\varphi$. This explains the observed dependence of the intensity of the Raman transition on the angle between pump and probe, and in particular the fact that Raman lines are not visible for small values of φ (Fig. 2).

3.3 Brillouin resonances

The Brillouin-like propagation modes in optical lattices have been first identified in reference [17] *via* semiclassical Monte Carlo simulations. They consist of a sequence in which one half oscillation in a potential well is followed by an optical pumping process to a neighbouring well, and so on (Fig. 5). The velocity of the Brillouin mode is easily calculated by neglecting the corrections due to the anharmonicity of the optical potential. The time for an atom to do half an oscillation is then $\tau = \pi/\Omega_x$. This corresponds to an average velocity

$$\bar{v} = \frac{\lambda_x/2}{\tau} = \frac{\lambda\Omega_x}{2\pi\sin\theta}\,. \tag{6}$$

The Brillouin mode is excited when the phase velocity of the moving modulation created by pump and probe is equal to the velocity of the Brillouin mode [17–19]. The condition $v_\phi = \bar{v}$ is written in terms of the detuning δ_{pc} between pump and probe as: $\delta_{pc} = \pm\Omega_\mathrm{B}$, with

$$\Omega_\mathrm{B} \equiv \frac{2\sin\varphi}{\sin\theta}\Omega_x. \tag{7}$$

Stimulated light scattering on the atoms following the Brillouin mode results in resonances in the probe transmission spectrum [15]. We claim that the resonances marked by an arrow on the spectra of Figure 2 are indeed *Brillouin resonances*. To verify that this is actually the case we studied the position of these resonances as a function of the light shift per lattice beam Δ_0' and as a function of the angle between pump and probe, with results as in Figures 6 and 7. The behaviour displayed by

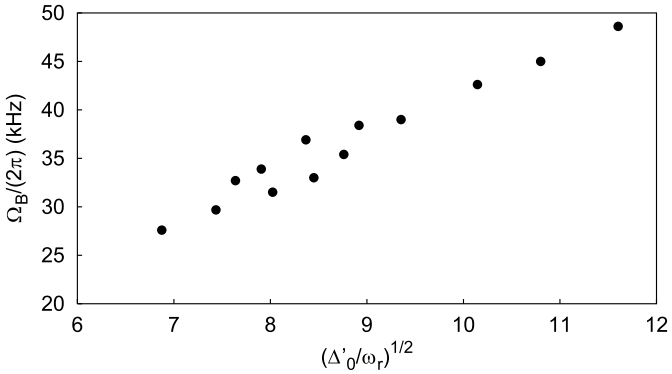

Fig. 6. Position of the Brillouin resonance as a function of the square root of the light shift per lattice beam Δ'_0 at a given angle between pump and probe ($2\varphi = 20°$). Here ω_r is the atomic recoil frequency.

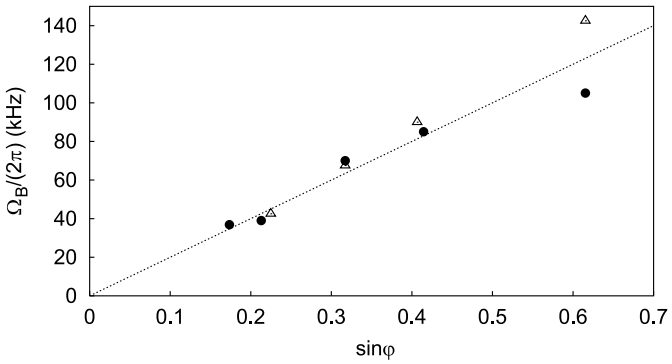

Fig. 7. Position of the Brillouin resonance as a function of $\sin\varphi$, where φ is the half-angle between pump and probe. The filled circles correspond to probe-transmission measurements, open triangles to the results of transport-spectroscopy. The dashed line corresponds to equation (7) with $\Omega_x = 2\pi\times 50$ kHz.

Figures 6 and 7 corresponds well to the dependencies of equation (7). Indeed the position of the resonances depends linearly on square root of the light shift per lattice beam, to which the vibrational frequencies are proportional, and on the sinus of the half-angle between pump and probe. We notice that this last property allows to clear distinguish the Raman and Brillouin resonances in the probe transmission. In fact, the positions of Raman resonances depend only on the lattice features (detuning, intensity and angle between the lattice beams), and not on those of the pump and probe beams.

4 Configuration with orthogonal pump and probe polarizations

We consider now the case of orthogonal pump and probe polarizations, with the pump field linearly polarized along y and the probe field in the xOz-plane. The displacement of the pump and probe beams is the same as in the configuration analyzed previously, the only difference being the polarization of the probe field.

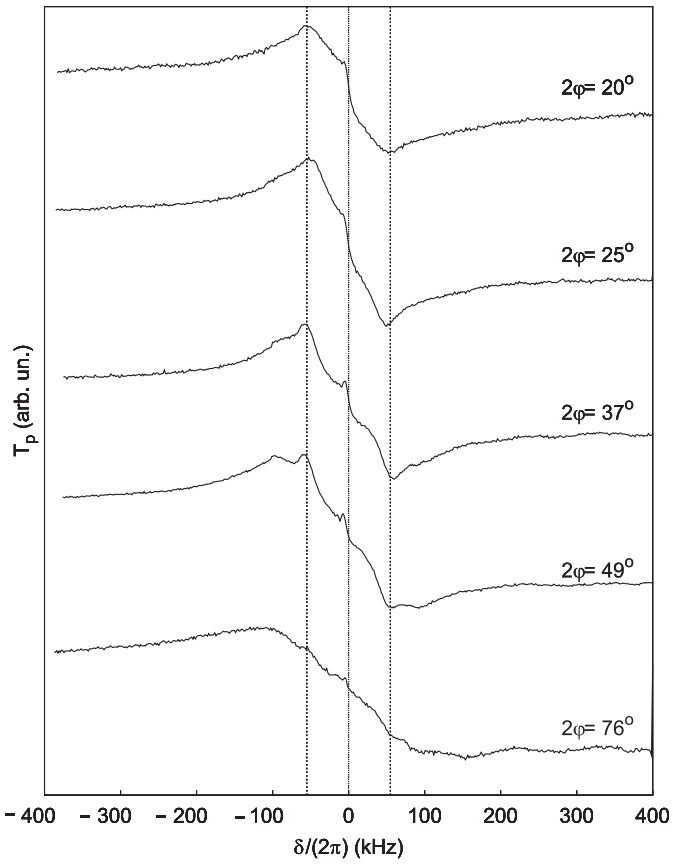

Fig. 8. Transmission of the probe beam as a function of the detuning between pump and probe fields, for different values of the angle 2φ between pump and probe beams. The lattice detuning is $\Delta = -50$ MHz, and the intensity per lattice beam $I_L = 5$ mW/cm^2.

Typical probe transmission spectra at different values of the angle 2φ between pump and probe beams are reported in Figure 8. Several resonances are present in these spectra. A narrow (few kHz) dispersive-like resonance centered at zero detuning is superposed to a broader (few hundreds kHz) resonance, also dispersive-like and centered at zero detuning. Two lateral resonances of opposite sign complete the spectrum.

Also for this pump-probe configuration we studied the velocity of the center-of-mass of the atomic cloud as a function of the detuning δ_{pc} and detected Brillouin propagation modes. However we found that for this pump-probe configuration these Brillouin modes do not produce resonances lines in the probe transmission spectrum and therefore they are not relevant for the present study. A complete account of these *dark* modes will be presented elsewhere [20].

4.1 Rayleigh resonances

The two dispersive-like resonances centered at $\delta_{pc} = 0$ correspond to stimulated Rayleigh scattering. They have respectively a width of few kHz and few hundreds kHz.

The mechanism behind these resonances is the same as for the configuration with parallel pump and probe: they originate from the diffraction of the pump on the phase-shifted modulation of an atomic observable. What differs in the two examined pump-probe configurations is the excited atomic observable. We have already discussed in Section 3.1 that for parallel polarizations of the pump and probe fields the modulated atomic observable assumed to be responsible for the Rayleigh line is the density. This density grating is created by the light intensity interference pattern via the dipole force. In the present case, the interference between the perpendicularly-polarized pump and probe gives rise to a moving pattern of the light polarization. Previous theoretical work (see [11] and references therein) identified in the atomic density and magnetization the material observable responsible for the Rayleigh line. In fact besides the obvious creation of an atomic magnetization grating, the modulated light polarization produces also a modulation of the depth of the optical potentials and therefore, *via* the dipole force, of the atomic density. As the two atomic observable (density and magnetization) have in general different relaxation rates, the time scale for the damping of the magnetization being shorter, the corresponding Rayleigh resonances have different widths, resulting in the observed structure in the probe transmission spectrum.

4.2 Raman resonances

The resonance at $\delta \simeq \pm 2\pi \times 50$ kHz are Raman resonances between different vibrational levels. To identify which mode is excited for a given pump-probe configuration and determine the dependence of the strength of the Raman lines on the angle between pump and probe, we proceed as in Section 3.2 and calculate the matrix elements of the Raman operator. The probe field has now components along the x- and z-directions. The field amplitudes in the two directions are $\mathcal{E}_{p,x} = \mathcal{E}_p^0 \cos\varphi$ and $\mathcal{E}_{p,z} = \mathcal{E}_p^0 \sin\varphi$. However, the component along the z-axis of the probe electric field cannot take part to a Raman process between ground states with the same m_g-quantum number because the pump field produces only $\sigma_\pm$ excitation with respect to the quantization axis (the z-axis). Through calculations analogous to those of Section 3.2, we get the following expression for the matrix-elements of the Raman operator

$$I_{nn'} \simeq \frac{(c_- - c_+)\mathcal{D}^2 \mathcal{E}_c^{0*} \mathcal{E}_p^0 \cos\varphi}{2(2J_e+1)} \langle \{n'\}|\mathbf{r}|\{n\}\rangle \cdot \Delta\mathbf{k}_{pc}. \quad (8)$$

We recognize in equation (8) the same type of coupling $\mathbf{r} \cdot \Delta\mathbf{k}_{pc}$ found for the case of parallel pump and probe polarizations. Therefore the conclusions of Section 3.2 for the correspondence between k-vector difference $\Delta\mathbf{k}_{pc}$ between pump and probe and the excited mode apply here as well. On the other hand, the dependence of the matrix-element $I_{nn'}$ on the angle φ is different from the case analyzed in Section 3.2. Indeed besides the term $\sin\varphi$ corresponding to $\Delta\mathbf{k}_{pc}$, in the present case there is an additional factor $\cos\varphi$. Therefore the strength of the Raman lines, proportional to $|I_{nn'}|$ varies as $\sin^2\varphi\cos^2\varphi$.

5 conclusions

In this work we described the pump-probe spectroscopy of atoms cooled in a 3D lin⊥lin optical lattice. Our pump-probe configuration consists of two laser fields detuned with respect to the lattice fields, at variance with previous investigations in which the lattice fields were playing the role of the pump and only one additional probe beam was introduced. This pump-probe configuration allows to clearly identify in the probe transmission spectrum the Brillouin and Raman resonances. We have shown that the different resonances can be distinguished by studying their positions as a function of the angle between pump and probe. The position of the Raman resonances corresponds to the energy spacing between vibrational levels, and does not then depend on the angle φ between pump and probe. By contrast, the position of the Brillouin resonances corresponds to a well defined velocity of the moving modulation created by the pump and probe beams. This velocity depends on the angle between the beams, and therefore also the position of the Brillouin resonances depends on the angle φ. This dependence has been verified in our experiment, with results in agreement with the theoretical model. Our conclusions have been supported by transport-spectroscopy measurements, which allow to distinguish between the contributions to the light scattering of propagating and non-propagating atoms.

This work was supported by the CNRS and the Région Ile-de-France under contract E.1220 "Atomes ultrafroids : vers de nouveaux états de la matière". Laboratoire Kastler Brossel is an "unité mixte de recherche de l'École Normale Supérieure et de l'Université Pierre et Marie Curie associée au Centre National de la Recherche Scientifique (CNRS)".

References

1. P. Verkerk, B. Lounis, C. Salomon, C. Cohen-Tannoudji, J.-Y. Courtois, G. Grynberg, Phys. Rev. Lett. **68**, 3861 (1992)
2. J.-Y. Courtois, G. Grynberg, Phys. Rev. A **46**, 7060 (1992)
3. J.W.R. Tabosa, G. Chen, Z. Hu, R.B. Lee, H.J. Kimble, Phys. Rev. Lett. **66**, 3245 (1991)
4. A. Hemmerich, T.W. Hänsch, Phys. Rev. Lett. **70**, 410 (1993)
5. J.-Y. Courtois, G. Grynberg, B. Lounis, P. Verkerk, Phys. Rev. Lett. **72**, 3017 (1994)
6. D.R. Meacher, D. Boiron, H. Metcalf, C. Salomon, G. Grynberg, Phys. Rev. A **50**, R1992 (1994)
7. F.-R. Carminati, M. Schiavoni, L. Sanchez-Palencia, F. Renzoni, G. Grynberg, Eur. Phys. J. D **17**, 249 (2001)
8. F. Chi, M. Partlow, H. Metcalf, Phys. Rev. A **64**, 043407 (2001)
9. G. Di Domenico, G. Mileti, P. Thomann, Phys. Rev. A **64**, 043408 (2001)

10. Y.-C. Chen, Y.-W. Chen, J.-J. Su, J.-Y. Huang, I.A. Yu, Phys. Rev. A **63**, 43308 (2001)
11. G. Grynberg, C. Mennerat-Robilliard, Phys. Rep. **355**, 335 (2001)
12. For a recent review of experiments on Bose-Einstein condensates in optical lattices, see O. Morsch, E. Arimondo, *Dynamics and Thermodynamics of Systems with Long Range Interactions*, edited by T. Dauxois, S. Ruffo, E. Arimondo, M. Wilkens, Lecture Notes in Physics (Springer, Berlin, 2002), Vol. 602
13. J. Dalibard, C. Cohen-Tannoudji, J. Opt. Soc. Am. B **6**, 2023 (1989); P.J. Ungar, D.S. Weiss, E. Riis, S. Chu, *ibid.* **6**, 2058 (1989)
14. Y. Castin, J. Dalibard, Europhys. Lett. **14**, 761 (1991)
15. J.-Y. Courtois, G. Grynberg, Adv. At. Mol. Opt. Phys. **36**, 87 (1996)
16. S. Guibal, C. Mennerat-Robilliard, D. Larousserie, C. Triché, J.-Y. Courtois, G. Grynberg, Phys. Rev. Lett. **78**, 4709 (1997)
17. J.-Y. Courtois, S. Guibal, D.R. Meacher, P. Verkerk, G. Grynberg, Phys. Rev. Lett. **77**, 40 (1996)
18. L. Sanchez-Palencia, F.-R. Carminati, M. Schiavoni, F. Renzoni, G. Grynberg, Phys. Rev. Lett. **88**, 133903 (2002)
19. M. Schiavoni, F.-R. Carminati, L. Sanchez-Palencia, F. Renzoni, G. Grynberg, Europhys. Lett. **59**, 493 (2002)
20. M. Schiavoni, L. Sanchez-Palencia, F.-R. Carminati, F. Renzoni, G. Grynberg, Phys. Rev. A (in press)